Civil and Architectural Engineering

Post-buckling Analysis of Cold-form Steel Column

Tuka Mohammed Qasim *
MSc. Student
Baghdad, Iraq
Tukam26@gmail.com

Salah Rohaima Al Zaidee
Assistant professor
Baghdad, Iraq
salahalzaidee2004@googlemail.com

ABSTRACT

$\mathbf{F}$or the time being, the cold-formed sections are widely used due to their simple manufacturing and construction processes. To be feasible, the strength of cold-formed columns should be determined based on their post-buckling behavior. Post-buckling relations are cumbersome and need design aids similar to those of American Iron and Steel Institute (AISI) to be applicable. These design aids have been developed to sections and materials other than those available in the local market. Therefore, this paper tries to develop a general finite element model to simulate the postbuckling behavior of cold-formed steel columns. Shell element has been used to discretize the web, flanges, and lips of the column. A linear bucking analysis with subspace Eigen value scheme has been achieved to determine the global, distortional, and local mode shapes. Subsequently, these modes have been used to generate the correspond imperfections. Finally, the modified Riks method has been used to solve the nonlinear equations of equilibrium and to a void the possible snap through phenomenon. Comparing with the traditional analyses using the effective width method and the direct strength method indicates that the finite element analysis is adequate and can be used for practical applications when dealing with local sections and materials.

Finally, different case studies with different column spans have been considered to show the behavior of the column for different slenderness ratios.

Keywords: Cold form steel, Column, Post-buckling.

تحليل ما بعد الانبعاج للاعمدة الحديدية المشكلة على البارد

صلاح رحيمه الزيدي
استاذ مساعد بروفسور

تقى محمد قاسم*
طالبة ماجستير

الخلاصة

في الوقت الحالي، يتم استخدام المقاطع المشكلة على الباردة على نطاق واسع بسبب سهولة تصنيعها و تشكيلها. لكي تكون مجدية ، يجب تحديد قوة الأعمدة المشكلة على أساس سلوكهم بعد الانبعاج. تعد علاقات ما بعد الانبعاج مرهقة وتحتاج إلى أدوات تصميم مماثلة لتلك الخاصة بـ AISI لتكون قابلة للتطبيق. لسوء الحظ ، تم تطوير أدوات التصميم هذه على مقاطع ومواد غير متوفرة في الاسواق المحلية. لذلك ، يحاول هذا البحث تطوير نموذج عام للعناصر المحددة لمحاكاة سلوك بعد الانبعاج للأعمدة الفولاذية المشكلة على البارد. تم استخدام عنصر القشرة لتقدير اجزاء العمود. تم إجراء تحليل ربط خطي باستخدام مخطط قيمة ايكن لتحديد

<div dir="rtl">

أشكال الانبعاج ان كان عام او تشويهي او محلي. بعد ذلك ، تم استخدام هذه الأوضاع لإنشاء عيوب المطابقة. أخيرًا ، تم استخدام طريقة ركس المعدلة لحل المعادلات التوازن الغير خطية ولتجنب ظاهرة المفاجئة المحتملة. تشير المقارنة مع التحليلات التقليدية باستخدام طريقة العرض الفعالة وطريقة القوة المباشرة إلى أن تحليل العناصر المحدودة مناسب ويمكن استخدامه للتطبيقات العملية عند التعامل مع المقاطع والمواد المحلية.

أخيرًا ، تم دراسة دراسات حالة مختلفة باستخدام أعمدة مختلفة الاطوال لإظهار سلوك العمود بالنسبة لنسب النحافة المختلفة.

الكلمات الرئيسية: الحديد المشكل على البارد، عمود، بعد الانبعاج

</div>

1. INTRODUCTION

Steel structures are manufactured from hot rolled sections or from cold form sections when the member is subjected to light loads or when the designer intends to use high efficient sections with high weight to strength ratio.

In cold-formed sections, the thickness of steel sheet or strip is between 0.378 mm to 6.35 mm. Steel plates and bars up to 25.4 mm may be bent and pressed successfully to form structural shapes. The Specification for the Design of Cold-Formed Steel Structural Members of the American Iron and Steel Institute (AISI) has been issued since 1946.

As the cold-formed steel member components are generally relatively thin with respect to their widths, they may buckle at stress value lower than the yield stress when it subjected to compression, shear, or flexure. Therefore, the major design consideration of the cold-formed steel members is the local buckling. It is well accepted that the cold-formed elements may not fail when it reaches to the buckling stress as they often will continue to support increasing forces that exceed the local buckling forces. In the post buckling stage, the load value may not change from the critical value or it may start to decrease while deformation is increase. Some cold-formed elements continue to support load after the deformation reaches to a certain value so the deformation is continuing to increase which finally cause a second buckling cycle. Therefore, the post buckling analysis is non-linear in nature and can provide more information than those obtained from a linear Eigen-value analysis **(Wei & Roger , 2010)**.

For cold-formed steel, there are three types of buckling modes namely the local buckling mode that involves web and flanges deformation without transverse deformation of the of the corners, the distortional buckling mode is similar to the local buckling mod but it involves the deformation of the corners, and flexural-torsional mode which do not change the cross section of the member and it can bend and twist see **Fig. 1** (Hancock, 2003).
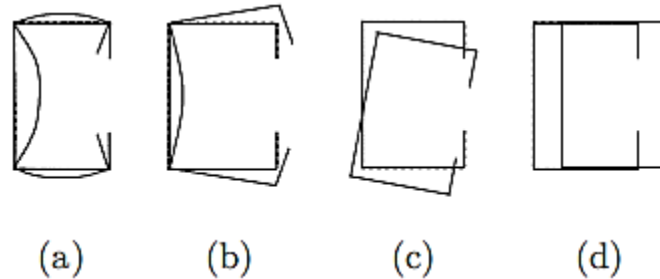

Figure 1. Lipped-channel column (a) local, (b) distortional, (c) flexural-torsional and (d) flexural buckling.

In post buckling behavior, the element may support additional load after buckling by a redistribution of stresses. This phenomenon is distinct for elements with high *W/t* ratios. As soon as the plate starts to buckle, the horizontal connected part will act as tie rods to inverse the increment in deflection of the member. The stress distribution that has been almost uniform before its buckling, as indicated in **Fig. 2a**, will be redistributed after buckling load in such a way that the center strip transfers to the edges as shown in **Fig. 2b**. The process continues until the stress of the edges reaches the yield stress and then the part begins to fail (**Fig. 3c**).
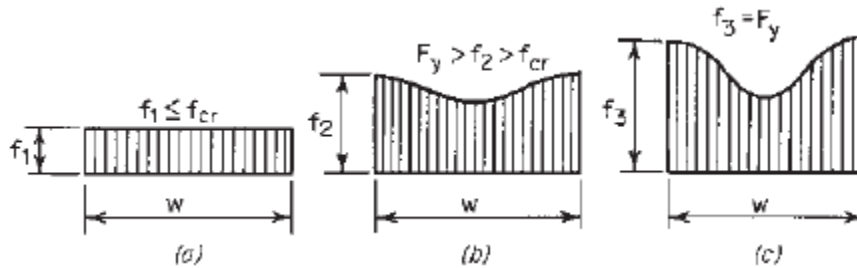
Figure 2. Consecutive stages of stress distribution in stiffened.

Large-deflection theory can be used to analyze the post buckling behavior through the following differential equation that introduced by von Karman in 1910:

$$f = \frac{\partial^4 \omega}{\partial x^4} + 2 \frac{\partial^4 \omega}{\partial x^2 \, \partial y^2} + \frac{\partial^4 \omega}{\partial y^4} = \frac{t}{D \left(\frac{\partial^2 F}{\partial y^2} \frac{\partial^2 \omega}{\partial x^2} - 2 \frac{\partial^2 F}{\partial x \, \partial y} \frac{\partial^2 \omega}{\partial x \, \partial y} + \frac{\partial^2 F}{\partial x^2} \frac{\partial^2 \omega}{\partial y^2} \right)} \qquad .....(1)$$

where F is a stress function expresses the median fiber stress. As the solution of this differential equation has little practical applications due to its complexity, a concept of effective width, b, has been introduced by von Karman et al. in 1932 to deal with a fictitious uniform stress instead of the actual non-uniform distribution over the whole width of the plate W. The value of the uniform stress has been taken equal to the edge stress f_{max}. The width b is selected such that the resultant for the actual non-uniform stress distribution to be equal to that of the equivalent uniform intensity **(Wei & Roger , 2010)**.

$$\int_0^w f \, dx = b \, f_{max} \qquad ....(2)$$

The Effective Width Method is available, all over the word to be used in the design. As an alternative analysis approach, the Direct Strength Method has been formally adopted in North American, Australia and New Zealand (Zheng, et al., 2012).

The effective cross-section illustrated in **Fig. 3a** provides a clear model for the effective and ineffective locations for carrying the load in the cross section, clues that the neutral axis changes its location in the section due to buckling. However, in the determination of the elastic buckling behavior it ignores the interaction and the compatibility, the overlapping of the buckling modes, like distortional buckling can be difficult to define, difficult and time-consuming iterations are required to calculate the member strength, and the evaluation of the effective section becomes more difficult if the section was complicated.

The basic idea of the Direct Strength Method is the exact member elastic stability, as shown in **Fig. 3b**. The determination of all elastic instabilities of section (i.e., local, distortional, and global buckling) and the yield load is the basic steps of the direct strength method. **(Schafer, 2006)**.

Elastic buckling is the load that the member equilibrium is neutral between the original deformed form and the buckling form. Elastic buckling evaluated in one of these methods: finite strip FS, finite element FE, generalized beam theory GBT, and closed form solutions. Finite strip analysis is a common method that determines precise values of elastic buckling with less effort and shorter time. FS analysis, adopted in the conventional programs like CUFSM, had a limitation that the

model assumes as a simply supported member of both ends and the cross-section is constant and do not change along the length. These limitations exclude some analysis from the real prediction using with the FS method, but notwithstanding these limits, the tool is useful (**American Iron and Steel Institute, 2006**).

A numerical investigation concerning the elastic and elastic–plastic postbuckling behavior of cold-formed steel lipped channel columns affected by distortional/global (flexural– torsional) buckling mode interaction was done by (**Dinis & Camotim, 2011**). A systematic investigation of material behavior, residual stress distribution, and axial compression performance on an extreme thick-walled cold-formed square columns which are manufactured from circular to square shape. was performed numerically and experimentally by (**Liu , et al., 2017**). (**Ma, et al., 2018**) presents the numerical investigation of the compressive behavior of cold-formed high-strength steel (HSS) tubular stub columns. An numerical investigation on slab-beam interaction in one-way systems presented by (**Al-Zaidee, 2018**). The strength of steel beam-concrete slab system without using shear connectors (known as a non-composite action), where the effect of the friction force between the concrete slab and the steel beam has been investigated, by using finite element simulation (**Al-Zaidee & Al-Hasany , 2018**)

In this paper, the researcher intends to study the postbuckling of cold formed steel columns using the finite element method by Abaqus which much easier and less time consuming and compare the results with the two other methods.
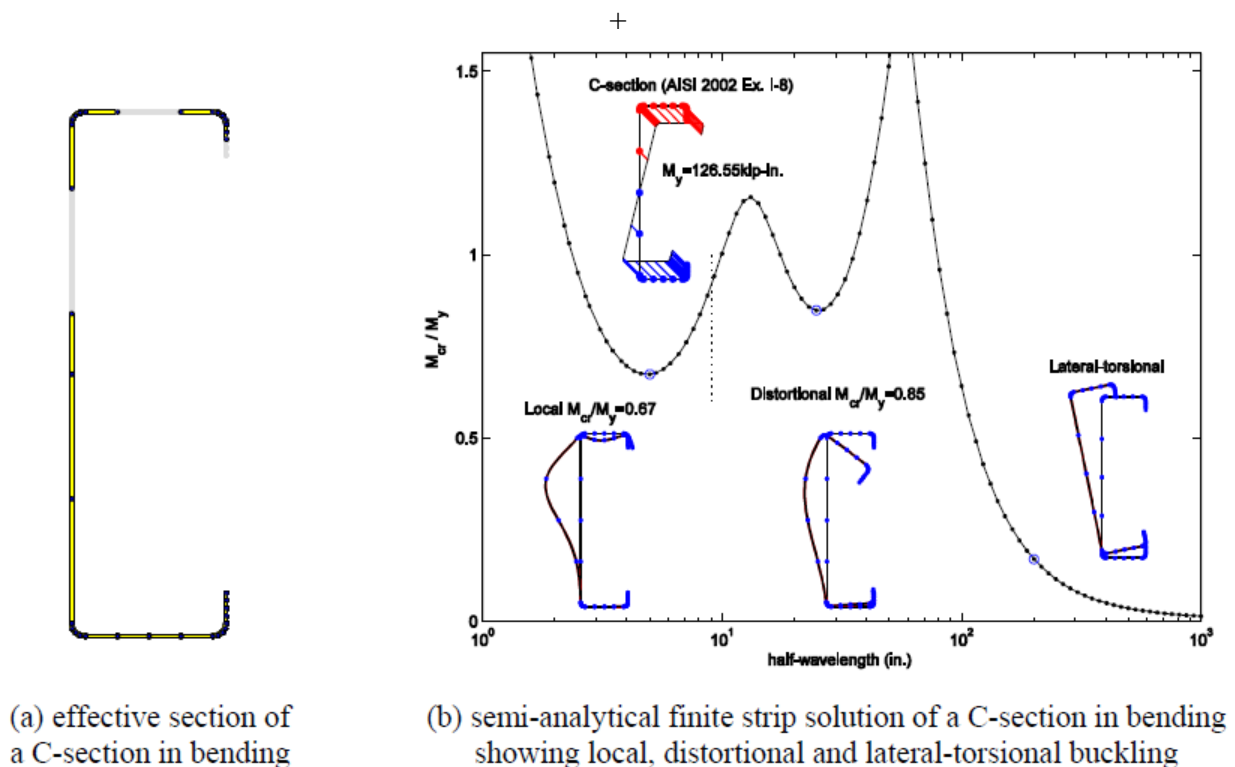

(a) effective section of a C-section in bending

(b) semi-analytical finite strip solution of a C-section in bending showing local, distortional and lateral-torsional buckling

Figure 3. Essential "thinking model" for (a) Effective Width and (b) Direct Strength Methods. (**Schafer, 2006**).

2. FINITE ELEMENT MODELING

In this section, a cold formed steel column 3m in length and with simple ends has to be analyzed using Abaqus software. It has been modeled with shell elements for its web and flanges. The geometrical properties, material properties, and the shell thicknesses have been defined as indicated in **Fig. 4**. The steel behavior is simulated as elastic perfectly plastic with yield stress equal to 355 MPa and modules of elasticity of 210000 MPa. A linear buckling load step has been defined to simulate the elastic buckling of the column. Assuming proportional loads, a unit shell edge load has been applied. Boundary conditions with $U_x, U_y,$ and $UR_z = 0$ have been assigned to both ends of the column. At the mid-span, the lateral movement has been prevented, $U_z = 0$, to restrain the rigid body motion.

The linear buckling analysis produces the Eigen value indicated in **Fig. 5** which represents the load multiplier necessary to produce the critical state. The critical axial force has been related to the Eigen value and the applied unit line load based on the following relation:

$$P = \frac{p}{t}A = 1 \times \frac{288.34}{2.4} \times 2.4\,(150 + 110 \times 2 + 17.5 \times 2) = 116.777 KN \qquad ....(3)$$
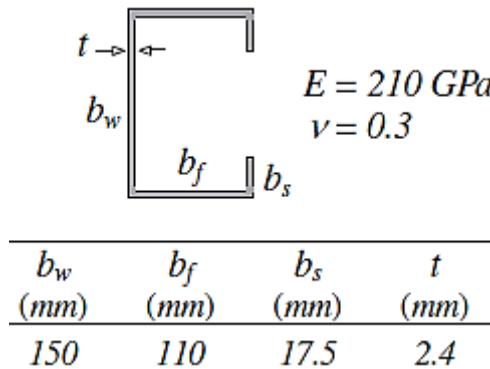

$E = 210\,GPa$
$v = 0.3$

b_w (mm)	b_f (mm)	b_s (mm)	t (mm)
150	110	17.5	2.4

Figure 4. Column dimensions and properties.

ODB: Colum   aqus/Standard 6.13-1   Sun Sep 02 17:15:21 Arabic Standard Time 2018
Step: Lin   Buckling
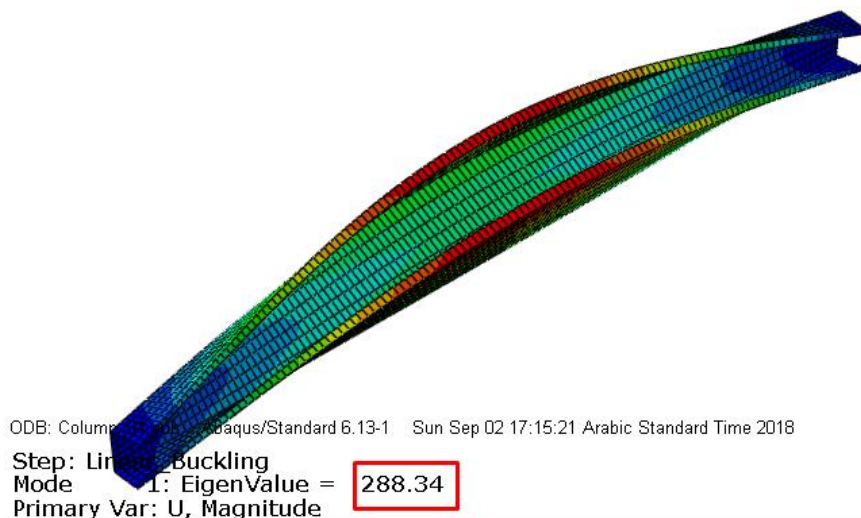Mode   1: EigenValue = 288.34
Primary Var: U, Magnitude

Figure 5. Eigen value of the finite element linear analysis.

177

To measure the post buckling behavior of the model, an imperfection of 3mm has been used to modify the mode shape of **Fig. 5** to simulate the imperfection along column length. The value of 3mm has been determined as $\ell/1000$ based on recommendations of **(Dinis & Camotim, 2011)** and **(Garifullina & Nackenhorstb, 2015).** The critical load from **Eq. (3)** has been applied and the model was analyzed. Static Riks non-linear analysis has been used to deal with the snap through the behavior of the post-buckling phenomenon **(Garifullina & Nackenhorstb, 2015).** Post-buckling analysis results are presented in **Fig. 6** which shows that the post-buckling behavior would be unstable at a critical load approaching 100 kN.
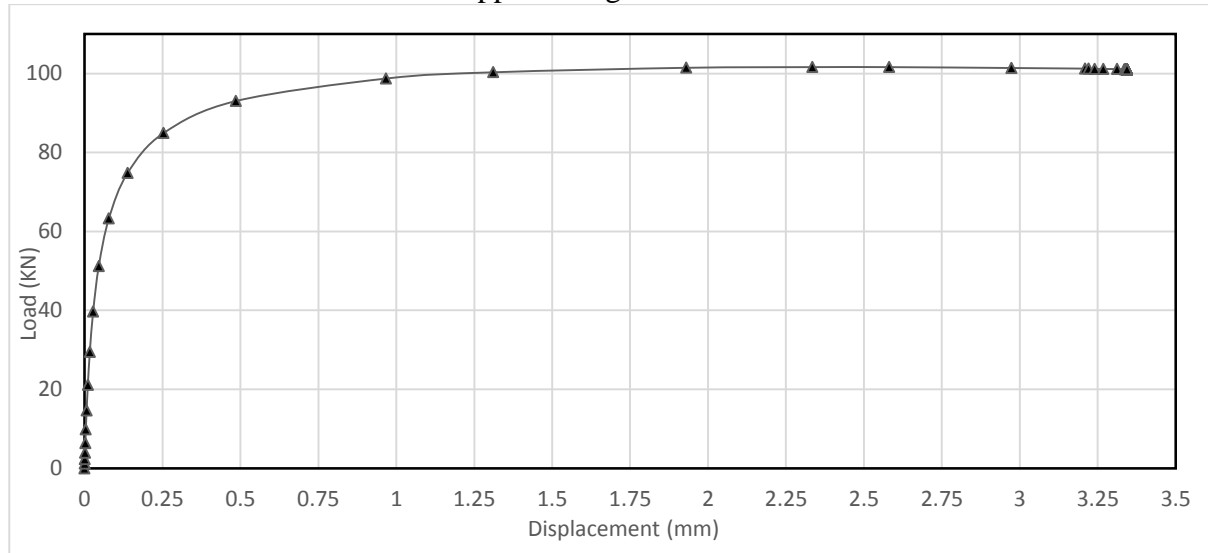

Figure 6. Load-displacement chart of the column.

3. VERIFICATION
The aim of this section is to compare the numerical postbuckling results of the Abaqus finite element analysis with those of the analytical buckling adopted by **(American Iron and Steel Institute , 2016)** and with those of the direct strength method using CUFSM software. The validation goals to prove the effectiveness of the finite element method in the analysis of this type of problems. The validated finite element model has the advantage over other analytical solutions in that it is general in nature and applicable for sections and materials other than those included in the manual.

3.1 Analytical Method
The analytical equations can be used to determine the post-buckling capacity of the cold-form columns. For a specific section with specific material properties, the global postbuckling axial strength can be determined based on **Eq. (4)** below.

$$P_{ne} = A_g F_n \qquad\qquad\qquad ….(4)$$

where:
A_g is the gross area, and F_n is the compressive stress that determined in below:

$$F_n = \left(0.658^{\lambda_c^2}\right)F_y \quad for \quad \lambda_c \leq 1.5 \qquad\qquad ….(5)$$

$$F_n = \left(\frac{0.877}{\lambda_c^2}\right) F_y \qquad for \quad \lambda_c > 1.5 \qquad \qquad ....(6)$$

where:

$$\lambda_c = \sqrt{\frac{F_y}{F_{cre}}} \qquad \qquad ....(7)$$

The F_y is yield stress while the F_{cre} is the least value of the elastic global (flexural, torsional, and flexural-torsional) buckling stresses. For singly-symmetric sections, such as Lipped C Channel of this study, that subjected to flexural-torsional buckling F_{cre} can be determined based on **Eq. (8)**:

$$F_{cre} = \frac{\sigma_t \sigma_{ex}}{\sigma_t + \sigma_{ex}} \qquad \qquad ....(8)$$

where σ_t is the stress due to Saint-Venant and warping torsions calculated from **Eq. (9)**.

$$\sigma_t = \frac{1}{Ar_0^2}\left[GJ + \frac{\pi^2 E C_w}{(K_t L_t)^2}\right] \qquad \qquad ....(9)$$

and r_0 is the polar radius of gyration of the cross-section about the shear center.

$$r_0 = \sqrt{r_x^2 + r_y^2 + x_0^2} \qquad \qquad ....(10)$$

r_x, r_y are radii of gyration of the cross-section about the centroidal principal axes in mm,
x_0 is the distance from the centroid to the shear center in principal axis direction in mm,
A is the full unreduced cross-sectional area of member in mm^2,
G is the shear modulus of steel MPa,
J is the Saint-Venant torsion constant of cross-section mm^4,
E is the modulus of elasticity of steel MPa,
C_w is the torsional warping constant of cross-section in mm^6,
K_t is the effective length factor for twisting,
L_t is the unbraced length of member for twisting in mm,
and σ_{ex} is the stress due to flexure calculated from **Eq. (11)**.

$$\sigma_{ex} = \frac{\pi^2 E}{\left(\frac{K_x L_x}{r_x}\right)^2} \qquad \qquad ....(11)$$

where:
K_x is the effective length factor for bending about x-axis,
L_x is the unbraced length of a member for bending about x-axis in mm,

For the section considered in this study, aforementioned section and material properties have been summarized in **Table 1**below.

Table 1 Geometrical and material properties of the section.

Variables	values
$A\ (mm^2)$	972
$G(MPa)$	80769.23
$J(mm^4)$	1866.24
$E(MPa)$	210000
$C_w(mm^6)$	7.6896×10^9
K_t	1
$L_t(mm)$	3000
$\sigma_t(MPa)$	137.058
$\sigma_{ex}(MPa)$	951.54

Then the critical stress will be $F_{cre} = 119.8\ MPa$ so compute λ_c from the **Eq. (7)** that $\lambda_c = 1.72 > 1.5$ so the compressive strength is calculated from **Eq. (6)** and $F_n = 105.24\ MPa$.Then the global buckling will be $P_{ne} = 102.3\ kN$

3.2 Direct Strength Method

The (**American Iron and Steel Institute, 2006**) has supported a research that led to the develop the CUFSM program, that depend on the FS method for elastic buckling calculation. This analysis two results have been provided: (i) the load-factors and the half-wavelength, and (ii) the buckling mode shapes. When CUFSM software was used to analyze different lengths of the cold-formed steel column of this study, it shows that:
- The global buckling occurs at a span length of about 2m,
- The distortional buckling dominates for spans between 0.3m to 2m,
- The local buckling occurs for spans less than 0.3m.

The elastic buckling strength for different spans has been presented in **Fig. 7**. The critical elastic loads for different zones have been determined as the minimum value for the corresponding zone. Then these critical elastic loads have been used in the empirical equations of the direct strength methods discussed in Section 3.2.1, Section 3.2.2, 3.2.3 to determine the corresponding post buckling loads. Analysis results including the elastic buckling loads and the post buckling loads (the nominal loads according to (**American Iron and Steel Institute, 2006**)) have been summarized in **Table 2**.

3.2.1 Global Buckling

The nominal axial strength, P_{ne}, for flexural, or torsional-flexural buckling is presented in **Eq. (12)** or **Eq. (13)**.

For $\lambda_c \leq 1.5$, Then $P_n = \left(0.658^{\lambda_c^2}\right)P_y$ ....(12)

Otherwise $\lambda_c > 1.5$, then $P_n = \left(\frac{0.877}{\lambda_c^2}\right)P_y$ ....(13)

where:

$$P_y = A_g F_y \qquad \text{....(14)}$$

where:
A_g: Gross area of cross-section in mm^2
F_y: Yield stress MPa

$$\lambda_c = \sqrt{\frac{P_y}{P_{cre}}} \qquad \text{....(15)}$$

where:
P_{cre} is the minimum of the critical elastic column buckling load in torsional-flexural buckling, N.

3.2.2 Local Buckling

The nominal axial strength bucking, $P_{n\ell}$,. for local buckling can be determined from **Eq. (16)** or **Eq. (17)** :

For $\lambda_\ell \leq 0.776$,Then $P_{n\ell} = P_{ne}$ ....(16)

Otherwise $\lambda_\ell > 0.776$,Then $P_{n\ell} = \left[1 - 0.15\left(\frac{P_{cr\ell}}{P_{ne}}\right)^{0.4}\right]\left(\frac{P_{cr\ell}}{P_{ne}}\right)^{0.4}P_{ne}$ ....(17)

where:

$$\lambda_\ell = \sqrt{\frac{P_{ne}}{P_{cr\ell}}} \qquad \text{....(18)}$$

where:
P_{ne} is the global column strength as defined in Section 3.2.1, N.

181

$P_{cr\ell}$ is Critical elastic local column buckling load, N.

3.2.3 Distortional Buckling

The nominal axial strength, P_{nd}, for the distortional buckling can be calculated in accordance with **Eq.(19)** or **Eq.(20)**.

For $\lambda_d \leq 0.561$,Then $P_{nd} = P_y$ **....(19)**

Otherwise $\lambda_d > 0.561$,Then $P_{nd} = \left[1 - 0.25\left(\frac{P_{crd}}{P_y}\right)^{0.6}\right]\left(\frac{P_{crd}}{P_y}\right)^{0.6} P_y$ **....(20)**

where:

$$\lambda_d = \sqrt{\frac{P_y}{P_{crd}}} \qquad\qquad ....(21)$$

where:

P_{crd}: Critical elastic distortional column buckling load, N.
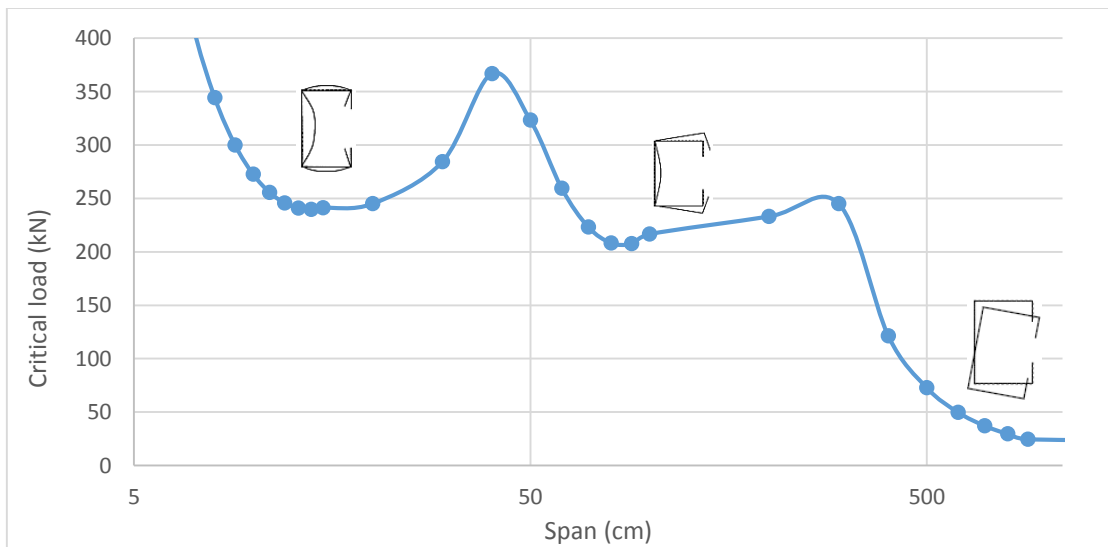

Figure 7. Finite strip analysis using the CUFSM software results.

Table 2 direct strength method results.

Buckling mode	Elastic buckling	Half wave length	Nominal buckling
	kN.	cm	kN.
Global buckling	245.0444	200	191.394
Distortional buckling	207.57	80	175.05
Local buckling	239.699	13	207.487

For this study with a span length of 3m, the buckling mode is a global buckling with an elastic buckling load of about 121 kN from **Fig. 7**. Using the global empirical equations of 3.2.1 the post buckling load would be 106 kN.

3.3 Results Discussion

The nominal axial strength of 101.65 kN from the finite element is close to, but slightly underestimated, the nominal strength of 102.3 kN from the analytical method. In percentage form, the difference between two methods is about 0.64%.

Comparing to the direct strength method, that has a nominal strength of 106 kN, the finite element solution seems more underestimated with a difference of 4.27%. The load-deflection curve of the post buckling finite element analysis with the nominal strength values form the analytical and direct methods have been presented in **Fig. 8**.

Aforementioned results and discussions indicate that the post bucking finite element analysis is fair accurate to be adopted in practical design especially when dealing with nontraditional dimensions and/or materials that have no analytical solutions.
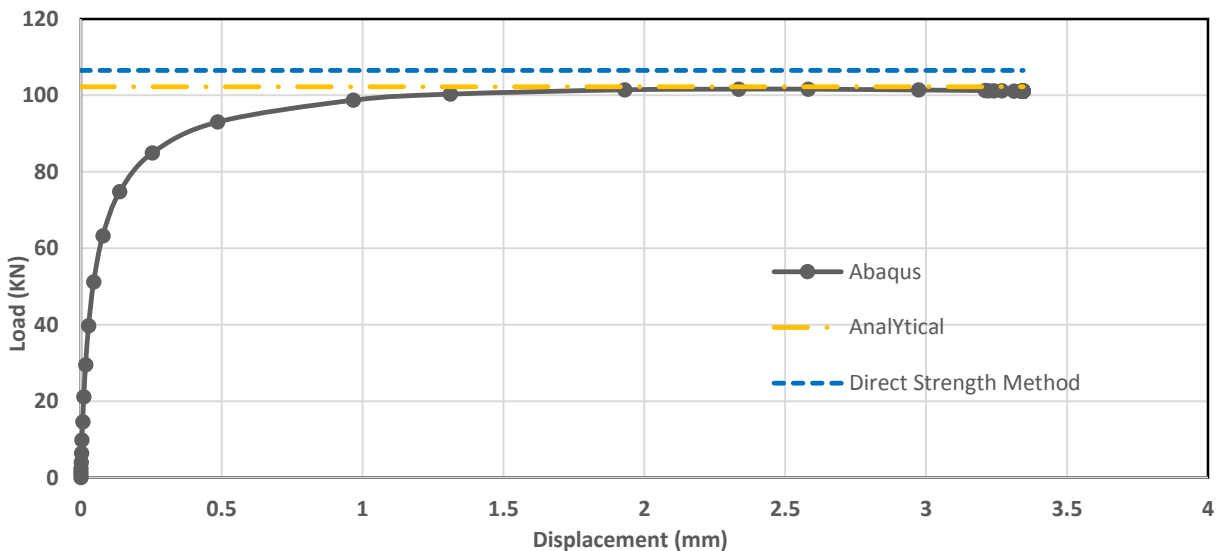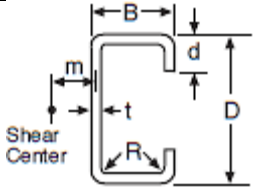

Figure 8: Load-deflection curve from the finite element post buckling analysis with the nominal strengths from the analytical and direct methods.

4. CASE STUDY

This case study adopts a cold-formed steel column from the (American Iron and Steel Institute, 2013) Manual with section of $8\,CS\,3.5 \times 0.085$ that has dimension and material properties indicated in **Table 3**.

Table 3. Column dimensions and material properties.

Dimensions and Material Properties in SI units	
Section depth D	$203.2\ mm$
Section width B	$88.9\ mm$
Section thickness t	$2.159\ mm$
Lipped length d	$21.2344\ mm$
Yield stress F_y	$379.2\ MPa$
Modulus of elasticity E	$199948\ MPa$
Poisson ratio v	0.3

A procedure similar to that adopted in Section 2 has been used in the case study of this section and other two sections that have the same dimensions but with thicknesses of 2.159,1.778 ,1.5 mm investigate different column lengths from 0.05m to 8.0m. Imperfections of $0.1t$ and $\ell/1000$ have been respectively adopted for the local and global buckling.

Results from the Abaqus finite element analysis have been gathered, organized, and presented in **Fig. 9** that shows three distinguished regions. In the first region, for short lengths up to 20cm, the local buckling is the dominate mode while the distortional bucking that is independent on the column length dominates the behavior from 20cm up to 200cm spans. Finally, the global mode governs the behavior of long columns with spans more than 200cm.

The section the that have a smaller thicknesses failed at lower load. The Sections have a nearly the same failure load in the global buckling region but they diverge in the local and distortional buckling zone.
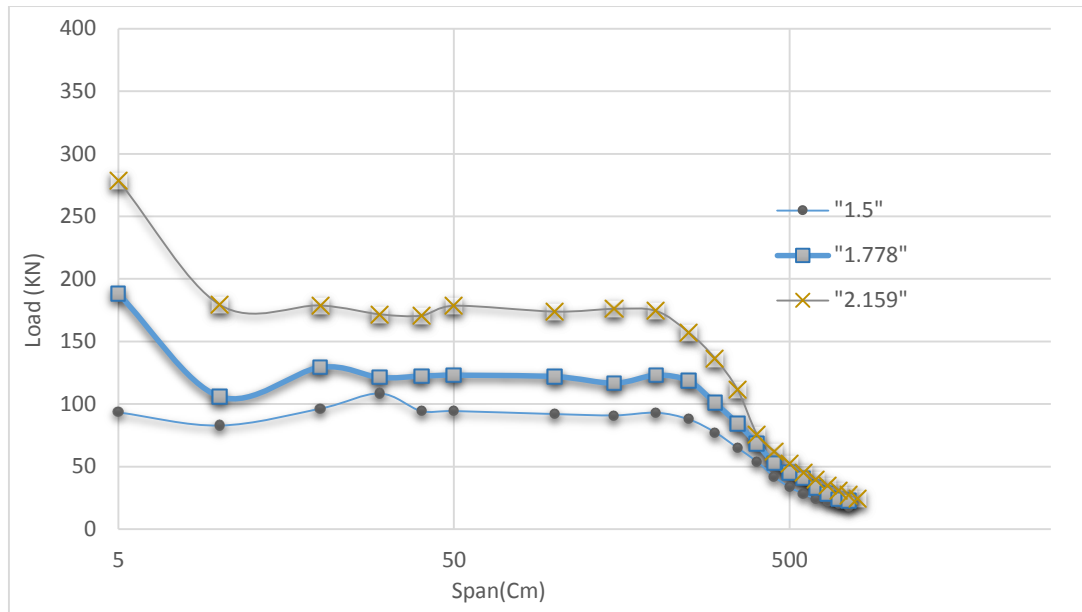
Figure 9. The effect of column length on buckling load.

5. CONCLUSIONS

Based on the aforementioned finite element modeling, solution processes, and the case studies the following conclusions can be drawn:

- Comparing with traditional analyses of the effective width method and the direct strength method, it has been found that finite element simulate can be adequate and conservative estimation of the post buckling strength of cold-formed steel columns.
- In addition to its validity, the finite element solution is a general in nature and can be adopted for sections and materials other than those of AISI design manual.
- The finite element solution can be used for different imperfection values that related to different buckling modes.
- Finally, the finite element solution can be used to study the behavior of cold-formed steel columns for different slenderness ratios.

RECOMANDATIONS

The following aspects that are significant from the subject point of view have not been discussed and they may be investigated in future works for a thorough understanding of the subject:

- Other cold-formed shapes such Z shape or hollow sections can be investigated.
- Inclined cold-formed sections can to be investigated.
- Effect of the vibrational aspects of the cold-formed steel column.

NOMENCLATURE

A : area, m^2.

A_g: Gross area, m^2.

C_w: Torsional warping constant of cross-section, mm^6.

E : Modulus of elasticity, MPa.

185

F_y: yield stress, MPa.
G: Shear modulus, MPa.
J: Saint-Venant torsion constant of cross-section, mm^4.
K: Effective length factor, unit less.
L: Laterally unbraced length of member, mm.
r: Radius of gyration of full unreduced cross-section about axis of buckling, mm.
r_0: Polar radius of gyration of cross-section about shear center, mm.
r_x, r_y: Radii of gyration of cross-section about centroidal principal axes, mm.
x_0: Distance from centroid to shear center in principal x-axis direction, taken as negative, mm.

REFRENCES

- Al-Zaidee, S. R., 2018. Slab-Beam Interaction in One-Way Floor System. *Journal of Engineering* , 24(3), pp. 122-134.

- Al-Zaidee, S. R. & Al-Hasany , E. G., 2018. Finite Element Modeling and Parametric Study on Floor Steel Beams Concrete Slab System in non composite Action. *Journal of Engineering,* 24(7), pp. 95-113.

- American Iron and Steel Institute , 2016. *AISI S100 Standard.* s.l.:AISI.

- American Iron and Steel Institute, 2006. *Direct Strength Method (DSM) Design Guide.* s.l.:American Iron and Steel Institute.

- American Iron and Steel Institute, 2013. *AISI Manual.* s.l.:AISI.

- Dinis, P. B. & Camotim, D., 2011. Post-Buckling Behaviour and Strength of Cold-formed Steel Lipped Channel Columns Experiencing Distortional/Global Interaction. *Computers and Structures,* Volume 89, pp. 422-434.

- Garifullina, M. & Nackenhorstb, U., 2015. Computational Analysis of Cold-Formed Steel Columns with Initial Imperfections. *Procedia Engineering ,* Volume 117, p. 1073 – 1079 .

- Hancock, G., 2003. Cold-formed steel structures. *Journal of Constructional Steel Research,* Volume 59, pp. 473-487.

- Liu , D., Liu, H., Chen, Z. & Liao, X., 2017. Structural behavior of extreme thick-walled cold-formed square Steel Columns. *Journal of Constructional Steel Research,* Volume 128, p. 371–379.

- Ma, J.-L., Chan, T.-M. & Young, B., 2018. Design of Cold-Formed High-Strength Steel Tubular Stub Columns. *Journal of Structural,* 144(6), p. 04018063.

- Reddy, J. N., 2004. *An Introduction to Nonlinear finite element analysis.* NewYork: Oxford University Press.

- Schafer, B. W., 2006. The Direct Strength Method of Cold-Formed Steel Member Design. *Stability and Ductility of Steel Structures.*

- Wei, W. Y. & Roger , A. L., 2010. *Cold-Formed Steel Design.* New Jersey: John Wiley & Sons, Inc., Hoboken.

- Zheng, S., Yang, Y. & Sun, D., 2012. Comparisons of EWM and DSM for Load-Carrying Capacity of Cold-Formed Lipped Channel Columns Under Axial Compression. *Advanced Materials Research ,* Volume 446-449, pp. 94-97.